

KINEMATICS ANALYSIS OF MAGNETIC ADSORPTION TUBE CLIMBING ROBOT BASED ON ADAMS

Yi Zheng^{1,2}, MingHua Liu¹, Jixin Liu¹, Shufang Zhou¹, Maohua Xiao^{1,3*}, Youqiang Wang^{2*}

¹Institute of Intelligence and Manufacture, Qingdao Huanghai University, Qingdao, 266427, China;

²School of Mechanical and Automotive Engineering, Qingdao University of Technological, Qingdao, 266520, China;

³College of Engineering, Nanjing Agricultural University, Nanjing 210031, China

*Correspondence: xiaomaohua@njau.edu.cn; Tel.: +86-13951756153

Email: littlsunny@sdust.edu.cn; Tel.: +86-15092153121

Abstract An articulated tube climbing robot with an adsorption device is designed to address the needs of the working environment outside pipeline tubes. The robot can perform actions such as walking on the tube, crossing obstacles, and rotating. A mechanism model is first established using SOLIDWORKS, and mechanical and finite element analyses are carried out to check the strength of the key parts and verify the rationality of the structure. ADAMS dynamics simulation of the tube-climbing robot outside the tube is then carried out, and the kinematic characteristics and data of the robot performing various actions through different pipelines are analyzed, providing a reference for the development of the prototype machine. The research results show that the mechanism design scheme of the tube climbing robot outside the tube is effective and reasonable.

Keywords: Tube Climbing Robot Outside The Tube; ADAMS; Simulation Analysis; Dynamic Simulation.

1. Introduction

Pipelines occupy an important position in industrial production and have a vital role in transporting fuels, chemical liquids, and toxic gases. Due to the danger of the substances inside the pipes, it is particularly important to ensure their safety and effectiveness. In the past, the daily inspection and maintenance of pipelines were carried out entirely manually, but the danger of the substances in the pipes made it extremely difficult for workers to work outside of the pipes. Therefore, with the development of the economy, the research and development of pipeline robots have gradually become significant [1-4].

This paper proposes a pipe-climbing robot that can adapt to changes in pipe diameter and move flexibly on the pipe. It is equipped with apparatus for work outside the pipe, which can meet the requirements for most of the work that is carried out.

This article first establishes a 3D model through SOLIDWORKS, which is then imported into ADAMS for simulation [5]. The ADAMS system outputs the kinematics simulation results to realize the kinematics research of the tube-climbing robot outside the tube and investigate the rationality of the structure design.

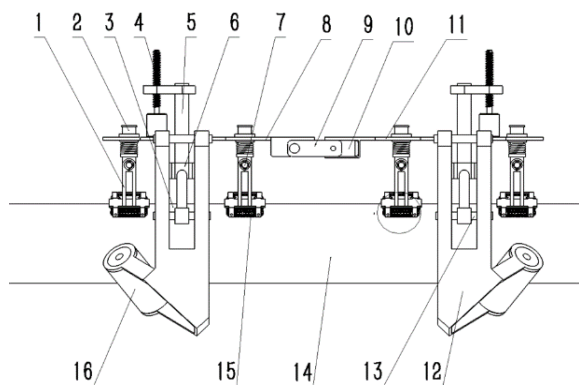
2. Model Establishment of Multi-functional Tube Climbing Robot

2.1 Institutional Analysis

A pipe climbing robot for work outside the pipe is designed in this work. The design structure is shown in Figure 1. The robot body is composed of two symmetrical front and rear parts. The front and rear frames are predominantly composed of a suction device and a holding and rotating device. The magnetic wheel in the suction device [6-7] is driven by a motor to realize the movement of the device on the pipeline. The screw rod is driven by the motor to rotate the lifting rod to move up and down. The bottom of the lifting rod is fixed to the push frame, and the push frame is connected to the steering wheel bracket so that the connected steering wheels on both sides of the pipe hold the pipeline tightly. This method only plays the role of auxiliary holding, and when the steering wheels on both sides turn in opposite directions, the device can be rotated around the pipe.

To ensure the reliability of the adsorption device, the three components (as shown in Figure 3) are arranged in a Y-shape (as shown in Figure 2) and are evenly distributed on the tube wall to maximize the effect of adsorbing the electromagnetic sheet.

The electromagnetic sheet adsorption is equidistantly embedded in the surface of the track, driven by the magnetic wheel, and energized when it is close to the target point. The power is turned off when it leaves the target point so as to realize the unity of the adsorption force and the forward driving force. When crossing obstacles and passing through special pipelines, the robot can be driven by a steering gear to flip the frame to complete the leaping action. The pipe-climbing robot studied in this paper is a magnetically attracted articulated pipe-climbing robot that can cross obstacles on the pipe, rotate around the pipe, and pass through various types of pipes.



1. Sub-adsorption bracket; 2. Main adsorption bracket; 3. Connecting rod; 4. Screw rod; 5. Lifting rod; 6. Pushed shelf; 7. Adsorption screw; 8. Front frame; 9. Frame with frame piece; 10. Steering gear; 11. Rear frame; 12. Steering wheel bracket; 13. Steering wheel bracket connecting rod; 14. Pipeline; 15. Cushion spring; 16. Steering wheel.

Figure 1: Two-dimensional front view of the tube climbing robot outside the tube.

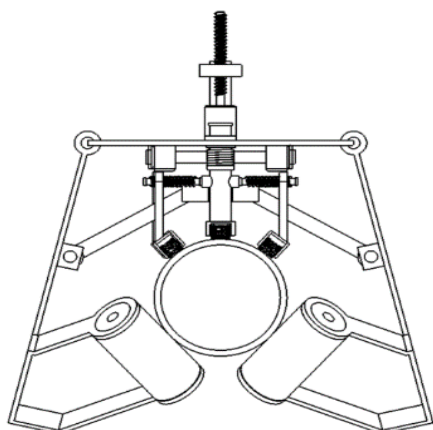


Figure 2: Two-dimensional side view of tube climbing robot outside the tube.

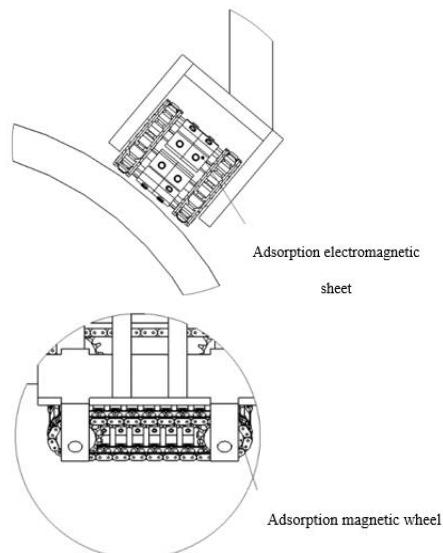


Figure 3: Two-dimensional schematic diagram of adsorption device

2.2 SOLIDWORKS 3D Model Establishment

The model of the SOLIDWORKS pipe-building and external pipe-climbing robot is shown in Figure 4 as a schematic diagram.

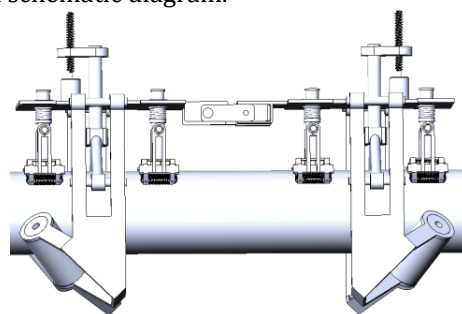


Figure 4: Three-dimensional model of the tube climbing robot outside the tube

3. Establishing the Robot Mechanics Model and a Finite Element Analysis of the Main Components

3.1 Mechanical Model Establishment

The tube-climbing robot proposed in this paper uses the principle of combined magnetic attraction and mechanical clamping to ensure the unity of flexibility and maneuverability of the entire mechanism. The mechanical model is shown in Figure 5.

In Figure 5, wheel 1 and wheel 2 are steering wheels, wheel 3, wheel 4, and wheel 5 are adsorption magnetic wheels, and the magnetic wheels are externally engaged with adsorption crawlers; N1 and N2 are the supporting force of the pipeline on the

two steering wheels (N); N₃, N₄, N₅, are the supporting force of the pipe to the adsorption device (N); F_A, F_B are the pipe wall friction force received by the two steering wheels (N); F₆, F₇ are the pulling force acting on the bracket of the two steering wheels (N); G is the gravity of the entire device (N); l₁ is the horizontal distance between the adsorption device and the pipeline centerline (mm); l₂ is the horizontal distance between the steering wheel and the pipeline centerline (mm); l₃ is the vertical distance between the support force N₃ and the support force N₁ (mm); A is the angle between the supporting force N₁ and the gravity (G); β is the angle between the friction force F_A and the gravity (G); γ is the angle between the friction force F_B and the gravity (G).

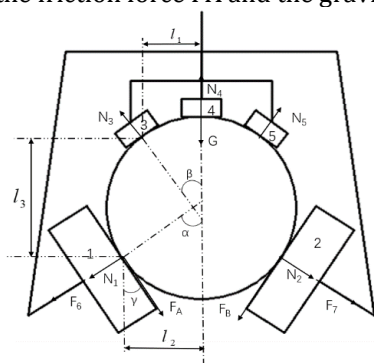


Figure 5: Clamping and adsorption force analysis model

The mechanical balance equations of the device are established for when the robot is in a state of uniform motion and in a state of equilibrium after being subjected to external forces [8]. The equations are as follows :

$$N_4 - G + (N_3 + N_5) \cos \beta - (N_1 + N_2) \cos \alpha - (F_A + F_B) \cos \gamma = 0 \tag{1}$$

$$(N_3 - N_5) \sin \beta + (N_1 - N_2) \sin \alpha + (F_B - F_A) \sin \gamma = 0 \tag{2}$$

$$(N_4 - G)l_2 + N_3 \cos \beta (l_2 - l_1) + (N_5 \cos \beta - N_2 \cos \alpha - F_B \cos \gamma)(l_1 + l_2) = 0 \tag{3}$$

$$(N_3 - N_5) \sin \beta l_3 = 0 \tag{4}$$

3.2 Force Analysis of Robot Adsorption Device

The outer wall of the tube is a curved surface, the robot crawls on the outer wall of the tube, and its working environment is a three-dimensional space. The top view of the robot working and crawling on the outer wall of the tube is shown in Figure 6. Among them, O is the center of the tube, R is the tube radius, B is the width of the adsorption device, n is the intersection between the left end of the

adsorption device, point O, and the outer wall of the tube, and α is the curvature angle of the robot.

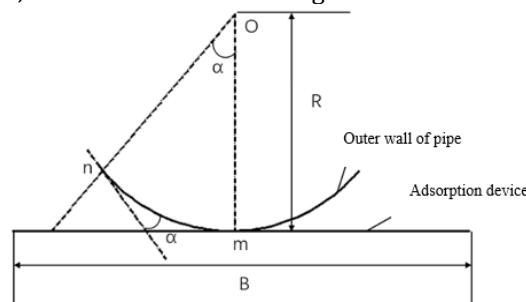


Figure 6: Top view of robot crawling

The outer diameter of the pipe used in this design is 4–6 m, and the width of the adsorption device is B = 50 mm. The calculation is based on Equation 5:

$$\alpha = \arctan \frac{B}{2R} = \arctan \frac{50}{4000} \approx 0.716^\circ \tag{5}$$

It can be seen from the analysis that the value of α is small and can be ignored, and as the outer diameter of the pipe increases, α shows a decreasing trend. Therefore, it can be simplified to a two-dimensional plane problem [9] in which the robot is approximated as working in a vertical plane. It is thus proven that the width of the current adsorption device can meet the hardware requirements for the robot to attach to the pipe wall.

3.3 Finite Element Analysis of Steering Wheel Support

The force analysis of the robot shows that its main force-bearing mechanism is the steering wheel support mechanism. Due to the influence of the clamping force and its own gravity, this support mechanism is prone to fatigue deformation, which has a significant impact on the work. Therefore, it must be calculated, checked, and modified to simulate the working condition with the greatest force.

The steering wheel bracket is made of high-strength 30Cr alloy, and the yield strength of the material can reach 685 MPa. The total gravity of the robot is 120 N, and it is loaded on the upper surface of the front and rear frames; the suction device is located below the center axis of the front and rear frames, and the suction force is loaded on the upper surface of the pipe. The left and right steering wheel brackets are hinged on the front and rear frames. It is necessary to carefully consider the transmission of force on both sides of the rear frame. The pipe is fixed, and the positive pressure from the pipe to the steering wheel is transmitted to the steering wheel support through the steering wheel. The suction magnetic wheel is driven by a motor, and the suction force of the suction device on the pipeline is transmitted to the steering wheel support through

the front and rear frame. Through the combination of SOLIDWORKS Motion and Simulation, the force information obtained is output through the

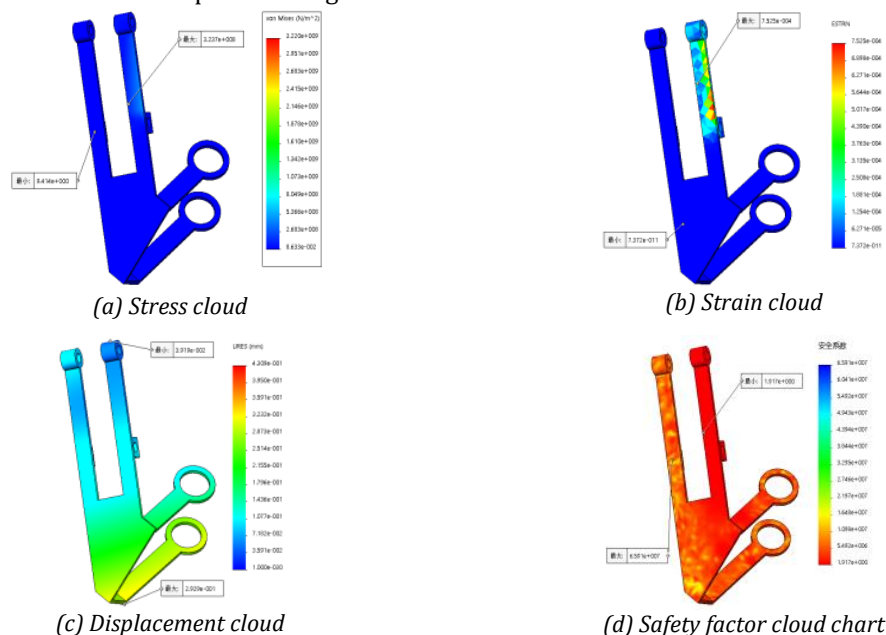


Figure 7: Finite element analysis results

It can be seen from Figure 7(a) that the maximum stress is 323.7 MPa, which is less than the yield strength of 30Cr. Figure 7(b) shows that the maximum strain is 7.52×10^{-4} . As illustrated in Figure 7(c), the maximum displacement occurs at the corner of the steering wheel bracket, and the value is 0.29 mm. It can be seen from Figure 7(d) that the minimum safety factor is 1.9, which demonstrates that the designed robot meets the strength requirements.

4. ADAMS Simulation Analysis

4.1 Model Assumptions

As the movement form and process of the pipe-climbing robot outside the pipe are more complicated, and the interaction between the joints inside the robot is difficult to accurately define, a flexible system model of the robot cannot be established [10]. Therefore, the following assumptions will be adopted in the study:

1) The robot only needs to calculate the contact friction between the suction device and the pipe wall, and all parts of the robot are rigid bodies with uniform masses.

2) Each electromagnetic adsorption sheet in each adsorption device is equivalent to a functioning adsorption sheet, and the acting direction is at the central axis of the adsorption device.

3) The resultant force experienced by the robot is equivalent to its center point, and its driving function is shown in the following formula:

Simulation function to the finite element analysis results, as shown in Figure 7.

$$\begin{aligned} \text{TraY: dip(time)} = & \text{step(time,0,0,5,5)} + \text{step} \\ & (\text{time},5,0,10,-5) + \text{step}(\text{time},10,0,15,5) \\ & + \text{step}(\text{time},15,0,20,-5) \end{aligned} \quad (6)$$

4.2 Virtual Prototype Creation

Motion simulation is performed on the 3D solid model assembled in SOLIDWORKS. The robot's motion mode and motion path is initially determined, saved in ADM format, and imported into ADAMS. After importing, the corresponding connection, force contact, and drive will appear in order to lay the foundation for simulation and post-processing. ADAMS then verifies that the model can move in accordance with the movement of the designed tube-climbing robot [11]. The ADAMS virtual prototype model of the established tube-climbing robot is shown in Figure 8.

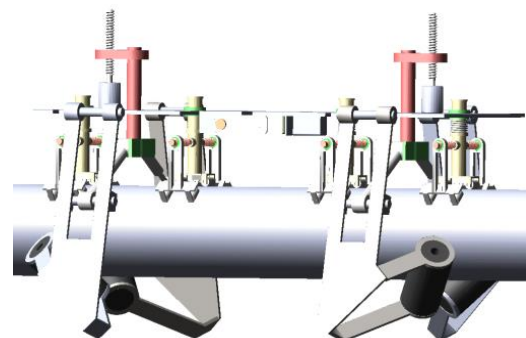


Figure 8: Virtual prototype model

The key to the design of a pipe climbing robot outside the pipe is to ensure that it moves linearly on the cylindrical pipe without rotating around the pipe due to unbalanced forces and to achieve the unity of adsorption and movement. To ensure these functions, the device is simulated and analyzed using ADAMS software [12-14], and it is first determined whether the component can meet the basic requirements for the robot to move linearly on the tube. It is then determined whether the component can meet the requirements of difficult movements, such as obstacle crossing by the robot on the tube. The ADAMS simulation analysis [15, 16] can also provide a foundation for further optimization in the future.

The robot's movement modes are determined as horizontal linear movement on a horizontal straight pipe, longitudinal linear movement on a vertical pipe, and movement when crossing obstacles.

4.3 Material Setting

The material, Poisson's ratio, and elastic modulus of each component is first obtained in ADAMS, and then the motion simulation is carried out. The materials table is shown in Table 1.

Table 1. Materials list

Components	Material	Poisson's ratio	Elastic modulus (MPa)
Pipeline	Iron	0.25	1.6×10^5
Wheel	Rubber	0.29	2×10^3

4.4 Linear motion simulation on the pipeline

The displacement, velocity, and acceleration of the robot are analyzed in three directions, and whether the motion state of the robot in the three-dimensional space meets the design requirements is investigated.

4.4.1 Linear motion simulation on horizontal pipelines

The motion requirements for the simulation of the robot on the horizontal straight pipe are:

- (1) Stable movement on the y-axis;
- (2) No displacement on the x and z axes and no movement up, down, left, or right.

ADAMS simulation is used to obtain the robot's displacement, velocity, and acceleration curve in the x, y, and z directions, as shown in Figure 9.

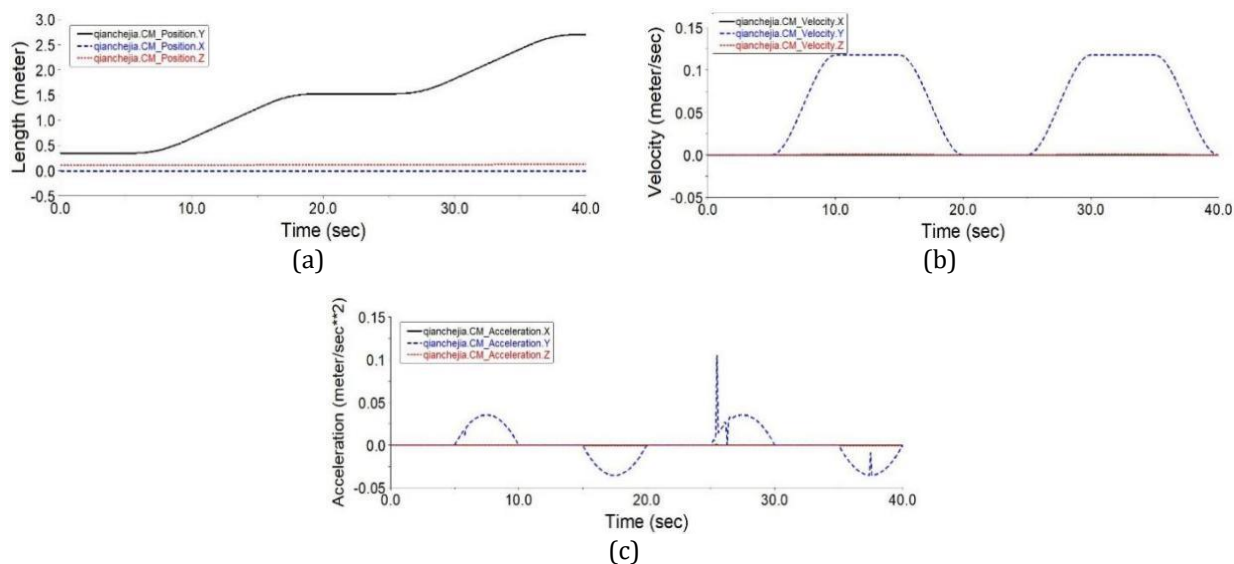


Figure 9: The robot's displacement, speed, and acceleration change curves in the x, y, and z directions

The displacement and speed of the robot in the three directions change with time (Figure 9(a),(b)). It can be seen that the x-axis and z-axis displacement and speed remain basically unchanged, indicating that the robot adsorption is basically stable.

There is also a situation of falling due to unstable adsorption; the y-axis demonstrates an obvious rising and steady state, the speed increases and

decreases relatively smoothly, and the maximum speed is maintained at 0.1 m/s, indicating that the robot can move smoothly on the wall.

The graph of the acceleration of the robot in the three directions with time (Figure 9(c)) shows that during the acceleration and deceleration process of the outer wall of the pipe, although the process fluctuates slightly, it is generally stable and is basically consistent with the speed change.

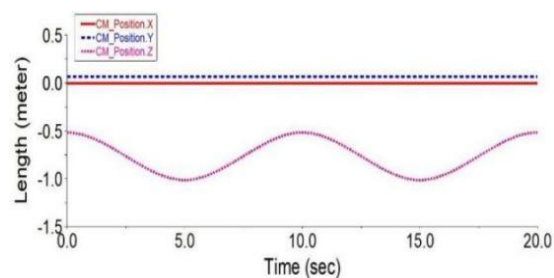
This proves that the working process of the robot conforms to the design plan and meets the expected design requirements.

4.4.2 Linear motion simulation on vertical pipes

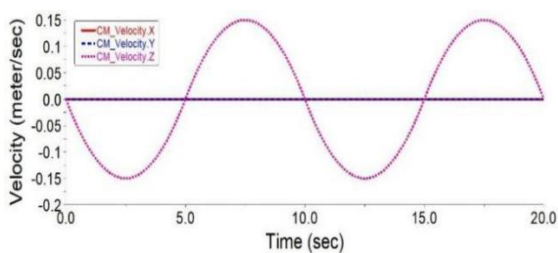
The movement on the vertical pipeline must resist the influence of gravity, as well as the combination of the adsorption and friction forces and the cooperation of the adsorption force and the adsorption device so that the robot can smoothly move in a straight line on the vertical pipeline. The driving function is as follows:

$$\begin{aligned} \text{TraZ:dip(time)} = & \text{step(time,0,0,5,5)} + \text{step} \\ & (\text{time},5,0,10,-5) + \text{step}(\text{time},10,0,15,5) \\ & + \text{step}(\text{time},15,0,20,-5) \end{aligned} \quad (7)$$

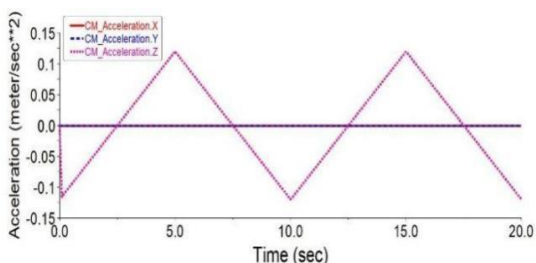
The movement situation is shown in Figure 10. It can be seen from the figure that the movement of the robot on the vertical pipeline meets the required smooth speed, and the maximum speed is 0.15 m/s, which meets the expected design requirements.



(a)



(b)



(c)

Figure 10: The robot's displacement, speed, and acceleration change curve in the x, y, z directions

4.5 Motion Simulation when Crossing Obstacles

Ten bytes is an important issue in the research of pipeline obstacle crossing. There are several methods to use ten bytes:

(1) Ten bytes perpendicular to the ground

As shown in Figure 11, from A to C, the device can go straight on the horizontal pipe, lift, adsorb, go straight on the vertical pipe, and drop several steps. From B to C, it can be rotated, go straight on the horizontal pipe, lift, adsorb, go straight on the vertical pipe, and drop several steps. The same goes for A to D and B to D, with the inclusion of rotation.

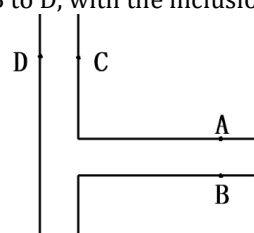


Figure 11: A schematic diagram of ten bytes perpendicular to the ground

(2) Ten bytes parallel to the ground

As shown in Figure 12, the robot can go straight from A to B, the front part can lift, and the front part can fall in the ten-byte position. The rear part can also lift, the front part can go straight on the horizontal pipe, and the rear part can fall. To reach point B from a position relative to A on the other side of the pipe, it will reach point A first after one rotation.

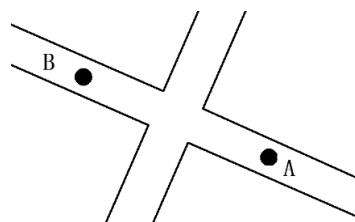


Figure 12: Schematic diagram of ten bytes parallel to the ground

Therefore, motion simulation analysis is predominantly conducted for lifting and rotating actions.

4.5.1 Motion simulation of lifting action

The speed change curve of the robot lifting is shown in Figures 13 and 14. The angular velocity changes smoothly, and the speed in the x-direction does not change, which proves that the adsorption force of the adsorption device is sufficient to keep the device stationary. The change in speed in the y-direction drives the entire device when the steering gear is activated.

When the gear sinks, the spring acts as a buffer, causing a slight fluctuation in the speed. The speed is within 0.01 m/s, and the whole lifting action takes 2 s to ensure the stability of the robot on the tube. As shown in Figures 15 and 16, the force of the front spring is different from that of the rear. The reason is that the pressure of the rear frame doubles when the front is lifted, so the two springs are subjected to more pressure at the back.

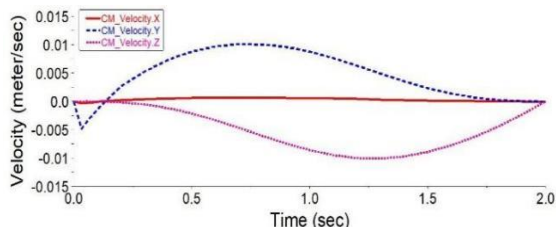


Figure 13: The speed cotton curve of the robot in the x, y, and z directions

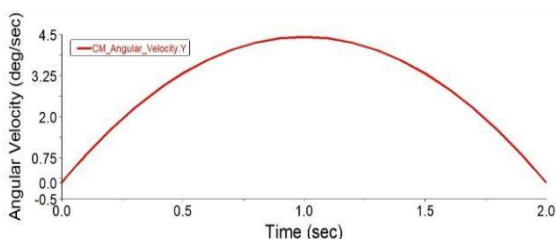


Figure 14: The angular velocity change curve of the robot in the y-direction

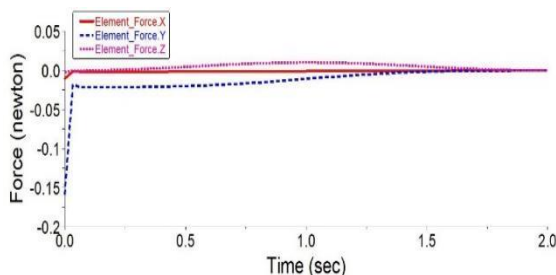


Figure 15: The force curve of the spring when the robot lifts up at the front

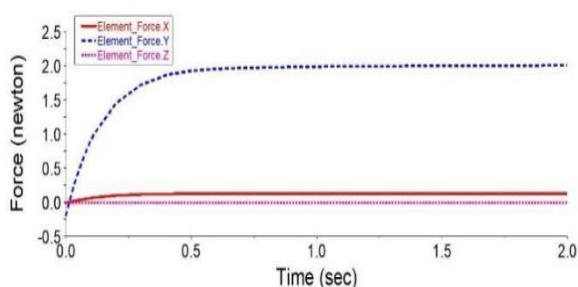


Figure 16: The force curve of the spring of the stationary part of the robot after lifting

4.5.2 Motion simulation of rotation

The speed change curve during the rotation process is shown in Figure 17. The image is recorded as one revolution, and the speed fluctuations are relatively large. Due to the influence of gravity, the

speed changes rapidly during the falling process. In the later stage of the rotation process, it is in the rising state, which is a process of slowing down. As shown in Figure 18, the spring is bullied by the force in the early fall process, which is similar to the speed curve, and the change tends to be gentler in the later stage of the rotation process. The overall speed and the spring force span are not large, which meets the design requirements.

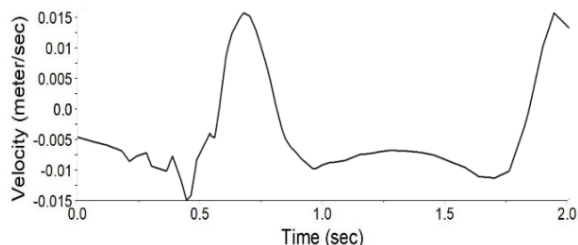


Figure 17: Speed curve

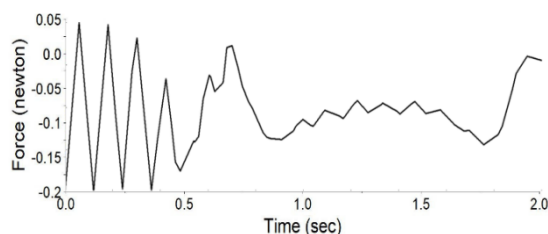


Figure 18: Spring force change curve

5. Conclusions

In this paper, an adsorption articulated pipe climbing robot was designed, which was modeled by SOLIDWORKS and imported into ADAMS for motion simulation. The simulation results showed that the pipe climbing robot had a reasonable structure and could achieve the required movement. According to the simulation of different actions of the robot and the investigation of various factors, it was concluded that the robot could proceed smoothly in a state of linear motion. It was also observed that certain problems in the robot motion simulation process remain for crossing obstacles, and further optimization and improvement are required. Through the joint simulation of SOLIDWORKS and ADAMS, the kinematic characteristics and data of the robot were obtained and provide a foundation for future prototype development and research.

Acknowledgements

This work was supported by Shandong Key Research and Development Project (No. 2019GHY112068), Qingdao postdoctoral applied research project (A2020-070) and the Natural Science Foundation of Shandong Province (No.ZR2020QE151)and Qingdao Huanghai University doctoral research Fund Project (2020boshi02).

References

- [1] Jang K Y., An Y K., Kim B H., et al. Automated crack evaluation of a high-rise bridge pier using a ring-type climbing robot. *Computer-Aided Civil and Infrastructure Engineering*, 2020, 36(1) : 14-29.
- [2] Zheng Y., Zhou S F., Deng C Y.. Optimization of the clamping mechanism for climb pipe joint type robot. *Journal of Mechanical & Electrical Engineering*, 2015,32(03):328-332.
- [3] Kermorgant O.. A magnetic climbing robot to perform autonomous welding in the shipbuilding industry. *Robotics and Computer Integrated Manufacturing*,2018,53.
- [4] Boomeri V. and Tourajizadeh H.. Design, Modeling, and Control of a New Manipulating Climbing Robot Through Infrastructures Using Adaptive Force Control Method. *Robotica*, 2020, 38(11) : 2039-2059.
- [5] Li Y X., Liu M L., Li X M.. ADAMS dynamics simulation analysis of pipeline detection robot. *Machinery Design & Manufacture*, 2020(10):243-247.
- [6] Santos H B.,Teixeira M A S.,Dalmedico N., et al. Model Predictive Torque Control for Velocity Tracking of a Four-Wheeled Climbing Robot. *Sensors*, 2020, 20(24) : 7059-7059.
- [7] Mayu S B. and Vidya P K.. Electrical Pole Climbing Robot for Fault Detection using Wi-Fi. *International Journal of Recent Technology and Engineering (IJRTE)*, 2020, 9(3):718-722.
- [8] Hernando M.,Gómez V.,Brunete A.,et al. CFD Modelling and Optimization Procedure of an Adhesive System for a Modular Climbing Robot. *Sensors*, 2021, 21(4) : 1117-1117.
- [9] Balan B.,Murali KB.,Niranjan M.,et al. Stair Climbing Robot using Star-Wheel Methodology. *International Journal of Recent Technology and Engineering (IJRTE)*, 2019, 7(6s5) : 1864-1866.
- [10] Wang Z Y.,Yang Y T.,Shang D S..Modeling and simulation of a six-legged high-rise building cleaning robot. *Manufacturing Automation*, 2019,41(08):64-67.
- [11] Schultz J T.,Beck H K.,Haagensen T.,et al.Using a biologically mimicking climbing robot to explore the performance landscape of climbing in lizards. *Proceedings of the Royal Society B: Biological sciences*, 2021, 288(1947) : 20202576-20202576.
- [12] Duan Y.,Hou Y.. The structure design and dynamic characteristics analysis of the wheeled pipe climbing robot. *Machinery Design & Manufacture*, 2016(12):17-20.
- [13] Bai Y., Jiang Q B., Mo L P., et al. Structural design and simulation analysis of hexapod bionic spider robot. *Journal of Mechanical & Electrical Engineering*, 2019,36(07):732-735.
- [14] Xu Y P.,Jordan M.,Johan T.,et al. Particles climbing along a vertically vibrating tube: numerical simulation using the Discrete Element Method (DEM). *Powder Technology*, 2017, 320 : 304-312.
- [15] Deeksha K.and Rajashekhar K P. . Reduction in climbing index of *Drosophila* revealed by Rotor-RING Assay suggests learned helplessness. *Journal of Entomological Research*, 2018, 42(2) : 271-274.
- [16] Wang W L.,Yang Q M,Sun C. Motion coordinated simulation and experimental study of dual-robot system . *Modular Machine Tool & Automatic Manufacturing Technique*, 2020(04):42-46.